

characteristics in the transition regime between free molecule and continuum flow," American Society of Mechanical Engineers Paper 63-WA-94 (1963)

⁵ Brown, G P, Di Nardo, A Chevy, G K, and Sherwood, T K, "The flow of gases in pipes at low pressures," J Appl Phys 17, 802-812 (1946)

⁶ Weber, S, "Über Den Zusammenhang Zwischen Der Lami-

naven Stromung Der Reinen Gase Durch Rohre Und Dem Selbstdiffusions-Koeffizienten, Math -Fysiske Meddelelser, Bind 28, no 2, 138-272 (1954)

⁷ Sparrow, E M and Jonsson, V K, "Free-molecule flow and convective energy transport in a tapered tube or conical nozzle," AIAA J 1, 1081-1087 (1963)

JUNE 1964

AIAA JOURNAL

VOL 2, NO 6

Fuel Containment in the Gaseous-Core Nuclear Rocket by MHD-Driven Vortices

JACOB B ROMERO*

The Boeing Company, Seattle, Wash

A gaseous fission propulsion engine is considered in which an electromagnetic vortex is employed for fuel retention. The pertinent continuity, momentum, energy, diffusion, and electromagnetic equations are derived for steady-state, laminar, two-dimensional flow and are solved for several cases. Economical fuel retention is considered from the point of view of rocket performance and design. Two basic design concepts are considered: a single critical chamber and multiple vortex tubes. Engine thrust-to-weight ratios range from ten-thousandths for the single vortex designs to tenths for the multiple vortex designs. Bypass flow systems are suggested as a means of obtaining performance improvement.

Nomenclature

B_0	= uniform axial magnetic flux density, webers/m ²
B_z	= axial magnetic flux density, webers/m ²
c_p	= gas heat capacity, joules/kg/°K
D_{12}	= diffusion coefficient of heavy gas in light gas, m ² /sec
E_r	= radial electric field strength, newtons/coul
H	= gas enthalpy, joules/mole
I	= radial current, amp/m
j_r	= radial current density, amp/m ²
k	= gas thermal conductivity, joules/m/sec/°K
K	= Boltzmann constant, joules/°K
L	= length of vortex, m
m	= mass of gas molecule, kg
m_T	= fuel mass inside chamber, kg
m_c	= critical mass, kg
N_{Pr}	= Prandtl number
n_p	= particle number density at r , number/m ³
N_{Re}	= radial Reynolds number
N_{Sc}	= Schmidt number
p	= gas pressure, newtons/m ²
P	= electric power loss, w/m
q	= conduction heat transfer, joules/sec/m ³
Q_f	= energy released per fission, joules
Q_v	= nuclear heat addition, joules/m ³
r	= radial distance (coordinate), m
r^+	= (r/r) , dimensionless radial distance (coordinate)
R	= universal gas constant, joules/kg/mole/°K
T	= gas temperature, °K
U	= potential drop across vortex, v
v_r	= radial gas velocity, m/sec
v_t	= tangential gas velocity, m/sec
w	= flow rate, kg/sec/m
Z	= axial distance (coordinate), m

σ_f	= fission cross section, m ²
μ	= gas viscosity, kg/sec/m
ω	= angular velocity, rad/sec
ρ	= gas density, kg/m ³
ρ^+	= ratio of fuel to propellant mass densities
σ	= gas electrical conductivity, mho/m
θ	= tangential coordinate
ϕ	= neutron flux, number/sec/m ²
Φ	= viscous heat dissipation, joules/m ³

Subscripts

1	= refers to species 1 or propellant
2	= refers to species 2 or fuel
m	= refers to position where the tangential velocity has a maximum
i	= refers to inner electrode outer radius
o	= refers to outer electrode inner radius

Introduction

PERFORMANCE of solid-core nuclear propulsion engines is limited by low maximum operating temperatures imposed by structural materials in the solid core. To overcome these temperature limitations, the gaseous-core nuclear propulsion engine has been suggested, in which both fuel and propellant are injected into the chamber itself, thereby avoiding major contact with structural surfaces and allowing higher temperature operation.

Unfortunately, loss of fuel in the rocket exhaust poses an equally difficult problem. The fuel loss is so great that, without some form of fuel retention, the gaseous-core engine is economically impractical. In order to solve this problem, several fuel retention schemes have been proposed¹⁻⁷. This paper discusses a few of these schemes and describes one, the MHD-driven vortex, in considerable detail.

In the MHD vortex, a uniform electric current flows between electrically insulated coaxial electrodes, and a magnetic field is applied axially. A partially ionized gas flowing uniformly between outer and inner electrodes receives a tangential force, thereby forming a vortex. High tangential velocities⁸⁻¹¹ that force the denser fuel to the chamber walls are im-

Received July 23, 1963; revision received March 4, 1964. The assistance of J C Almond and D E Heard with the computer calculations is gratefully acknowledged. Barbara Romero assisted in typing the rough manuscript. Assistance in preparing and arranging the final manuscript and graphic art was rendered by G L Case, N E Evans, H T Martin, P C Canup, and H J Mosich of the Boeing Audio Visual Support and Publishing Section.

* Lead Engineer, Advanced Nuclear Group. Member AIAA.

parted to the gas, thereby preventing fuel-rich gas from being exhausted from the rocket

The primary advantage of the electromagnetic vortex concept lies in forming the vortex independently, whereas, for example, in the hydrodynamic vortex concept^{1, 2} the fluid is introduced tangential to the chamber wall, thereby forming its own vortex. Mass flow rate per unit of chamber length is independent of vortex diameter and is limited primarily by maximum tangential Mach number, an obvious disadvantage in the hydrodynamic vortex since the vortex strength depends on the flow rate.

Rocket Engine Characteristics

Engine Design Considerations

One type of MHD vortex rocket-engine concept is the single, reflected chamber design shown schematically in Fig 1. The propellant with makeup fuel cools the walls, enters the chamber through the outer wall, diffuses through the fuel-rich cloud, and exits to the nozzle. The electrical current flows between the outer wall and the central electrode, and the axial magnetic field is produced by the solenoid.

The second reactor design considered consists of many small vortex tubes packed in a large reflected chamber. Two concepts, consisting of 1000 and 3000 individual tubes, were studied. This design, in effect, increases the over-all vortex length and has been suggested as a means of increasing the total flow rate in hydrodynamic vortices.² In both single and multiple designs, a vortex radius ratio (r/r_i) of 10 was used. Calculations show that, as this parameter is decreased, larger electrical powers are necessary to maintain the same tangential velocity. The value of 10 is consistent with nozzle design and maintains high tangential velocity with reasonable power.

The inner electrode is shown in Fig 1 as a perforated cylinder through which the hot gases exit, mainly to indicate the concept without considering specifically such problems as wall cooling or fuel condensation. The environment in which this electrode is located is severe, and in actual practice some other method, if workable, would be superior. The best alternate would be to use the hot gas itself as an electrode. This scheme has been used in such devices as Ixion,¹² but its practicality has yet to be verified for the conditions encountered in gaseous reactors. A second alternate might be to use a consumable electrode of the ablative type. Some electrodes of this type are used in plasmajets, but require analysis in applications to gaseous reactors for factors such as heat transfer, nucleonics, and electromagnetic effects. For the present study, which is concerned primarily with containment feasibility and preliminary design, an electrode of constant dimensions with uniform current and gas flow is assumed.

The criticality of the reactor depends on the fuel used and on the nature and thickness of the reflector. The reactor envisioned is of the externally reflected type in which a reflector surrounds the reacting cavity. To conserve neutrons, a reflector of considerable thickness is necessary; this dictates, to a large extent, dead reactor weight (all weight except that of electrical power equipment). The two designs used here assume a cavity of 2-m radius and are reflected by 0.55 m of heavy water on all sides. The electrical insulators between electrodes can also be used as reflectors by constructing them of heavy water contained in an electrical insulator. The critical mass of Pu-239, needed for criticality in these reactors, is about 8 kg.¹³ However, to account for the effects of nozzle, pressure shell, geometry, and impurities, a critical mass of 10 kg was assumed as reasonable in the calculations. This gives an over-all average fuel density of about 0.4 kg/m³. Increasing fuel containment beyond this value does not drastically increase the electrical requirements because it is shown later that the $B_0 I$ product does not change greatly.

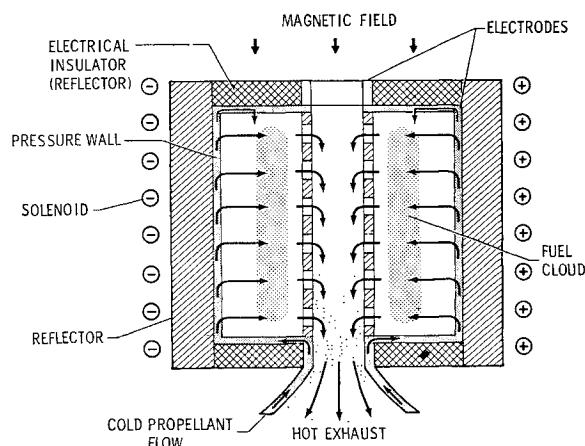


Fig 1 Gaseous nuclear rocket concept

Typical dead weights for a 2-m-length reactor are 92,000 lb of heavy water, 5000 lb of pressure shell, and 1000–2000 lb for the nozzle, pump, accessories, and solenoid. From these values, it can be seen that the reflector requirements dominate. An over-all reactor dead weight of 50,000 lb/m was used in computing engine performance.

Mathematical Formulation

Major Assumptions Used

To simplify the mathematics, the problem of containment was treated in a simplified manner. Figure 2 shows the simplified two-dimensional vortex studied. Flow and current were assumed to move uniformly between electrodes, and the system was assumed axially symmetrical—all quantities independent of θ . A uniform magnetic field was assumed to act axially. Further assumptions made were the following:

- 1) The electron free path is much less than a typical dimension of the plasma volume. This assumption is basic to the application of the continuum equations. At the plasma pressures of interest to propulsion, this assumption should hold quite well.
- 2) The magnetic Reynolds number is much less than 1. For this case, the Hall currents can be neglected, and the axial magnetic field is approximately constant: $B = B_0$.
- 3) The flow is laminar. This assumption is probably erroneous; turbulent flow has been shown to be predominant in jet-driven vortices. However, in the MHD-driven vortex, the magnetic field tends to stabilize turbulence, and it might be possible to extend laminar conditions to higher velocities.
- 4) The flow is two-dimensional. This assumption also is probably erroneous; three-dimensional effects have been shown to exist in jet-driven vortices. By special design, two-

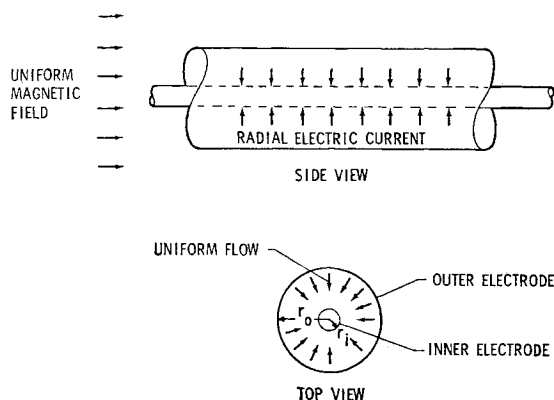


Fig 2 Two-dimensional MHD-driven vortex

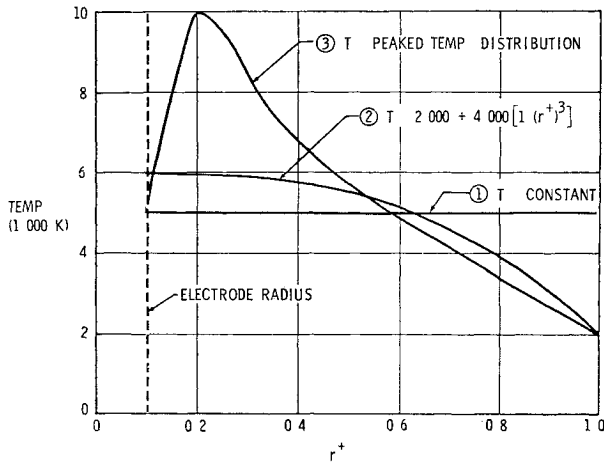


Fig 3 Temperature distributions studied.

dimensional flow can probably be approached, although total two-dimensionality may be impossible to achieve

5) The concentration of one species (propellant) is so prominent that the gas transport properties, except electrical conductivity, can be assumed to be those of this species. Nucleonics data indicate that, for critical systems, this assumption is approached (i.e., $n_{p2} \ll n_{p1}$)

Diffusion

The equation governing radial diffusion of a binary mixture may be found in Ref. 14. Neglecting the effect on diffusion of external forces and temperature gradients, the diffusion equation has been written in Ref. 15 as

$$1 - \left(\frac{1 + \rho^+}{\rho^+} \right) \left(\frac{w_2}{w_1 + w_2} \right) = \frac{-2\pi\rho_1 D_{12}}{w_1 + w_2} \left[\frac{d \ln \rho^+}{d \ln r} - \left(\frac{m_2}{m_1} - 1 \right) \frac{v_t^2}{RT} \right] \quad (1)$$

by employing the continuity and radial momentum equations. In this equation, the particle concentrations have been expressed, for convenience, in terms of density ratio defined as $\rho^+ = \rho_2/\rho_1 = m_2 n_{p2}/m_1 n_{p1}$

Equation (1) is complicated by the fact that v_t and T are functions of radius. ρ_1 and D_{12} are functions of temperature and, thus, of radius. A great deal of simplification is possible if the dependence of viscosity on temperature is neglected. This allows the definition of a radial Reynolds number and Schmidt number which may be assumed constant. Over the kinetic range, viscosity varies with the square root of the temperature, and the variation is, therefore, relatively weak. As an approximation, it will be assumed that viscosity can be represented as an average value calculated at the average temperature.

The final form of the diffusion equation can now be written as

$$\frac{d\rho^+}{dr^+} + \left[N_R N_{Sc} \left(\frac{w_2}{w_1 + w_2} \right) - N_R N_{Sc} - \left(\frac{m_2}{m_1} - 1 \right) \frac{v_t^2}{RT} \right] \frac{\rho^+}{r^+} + N_R N_{Sc} \left(\frac{w_2}{w_1 + w_2} \right) \frac{1}{r^+} = 0 \quad (2)$$

where a radial Reynolds number is defined as $N_R = -(w_1 + w_2)/2\pi\mu$, and a Schmidt number for the light gas is defined as $N_{Sc} = \mu_1/\rho_1 D_{12}$. For convenience, a reduced coordinate defined as $r^+ = r/r_0$ has been used.

Velocity Distribution

The rotational velocity of the plasma for the case considered is found from the θ components of the momentum equation

using a procedure which differs from that of Gordeev and Gubanov⁸ only in the introduction of the radial velocity. The resulting differential equation can be written as

$$\mu \left(\frac{d^2 v_t}{dr^2} + \frac{1}{r} \frac{dv_t}{dr} - \frac{v_t}{r^2} \right) = j B_0 + v_r \rho \left(\frac{dv_t}{dr} + \frac{v_t}{r} \right) \quad (3)$$

Combining Eq. (3) with the continuity equation for the gas mixture and assuming uniform radial current, the result can be reduced to

$$r \frac{d^2 v_t}{dr^2} + (1 - N_R) \frac{dv_t}{dr} - (1 + N_R) \frac{v_t}{r} = \frac{B_0 I}{2\pi\mu} \quad (4)$$

where $j_r = I/2\pi r$. I is the current per unit length.

When no electromagnetic field is present, the right-hand side of Eq. (4) vanishes and the equation corresponds to that obtained for a hydrodynamic vortex.

Equation (4) is a Euler equation solved for the boundary conditions $v_t = 0$ when $r = r_i$ and r , yielding the result

$$v_t = - \frac{B_0 I r_0 r^+}{4\pi\mu N_{Re}} \left[1 - K_1 \left(r^+ \frac{r_0}{r_i} \right)^{N_R} - K_2 \left(\frac{1}{r^+} \right)^2 \right] \quad (5)$$

where

$$K_1 = [1 - (r/r_i)^2]/[1 - (r/r_i)^{N_R+2}]$$

$$K_2 = [1 - (r/r_i)^{N_R}]/[1 - (r/r_i)^{N_R+2}]$$

and a reduced radius is again used. Letting $N_R \rightarrow 0$, Eq. (5) reduces to the solution obtained by Gordeev and Gubanov⁸ for stationary flow.

The maximum velocity also may be found by setting the first derivative to zero. This occurs at the radius computed from the following complicated polynomial

$$(r_m)^{N_R} \frac{(1 + N_{Re})K_1}{(r_i)^{N_R}} = 1 + \frac{K_2 r_0^2}{r_m^2} \quad (6)$$

Pressure Distribution

The radial pressure distribution is found from the radial momentum equation. As in Ref. 2, this can be expressed approximately for the case where $v \ll v_t$ by the equation

$$\frac{dp}{dr^+} = \frac{m_1}{K} (1 + \rho^+) \frac{v_t^2 p}{r^+ T} \quad (7)$$

This equation can be integrated readily to

$$\frac{p}{p_i} = \exp \frac{m_1}{K} \int_{i^+}^1 \frac{(1 + \rho^+)}{T} \frac{v_t^2}{r^+} dr^+ \quad (8)$$

Energy Equation

The energy equation for the two-dimensional system considered, neglecting radiation, can be written as

$$\rho v \frac{dH}{dr} = v \frac{dp}{dr} - \frac{1}{r} \frac{d}{dr} (r q) - \frac{j^2}{\sigma} + Q + \Phi \quad (9)$$

Equation (9) is the usual two-dimensional equation in cylindrical coordinates with electrical and fission heating terms included.

Using the approximations suggested by Kenebeck and Meghieblan² for enthalpy, thermal conductivity, and fission heating, the expression for viscous dissipation for the case $v \ll v_t$ (Ref. 9), the radial momentum equation, and Eq. (5), the energy equation reduces, after some manipulation, to

$$\frac{d^2 T}{dr^2} + (1 - N_R N_P) \frac{1}{r^+} \frac{dT}{dr^+} + \frac{m_1 Q_f \sigma_f \phi r_0^2}{K m_s k} \rho^+ \times \\ (1 + \rho^+) \frac{p}{T} + \frac{N_{Re} N_{Pr}}{c_{p1}} \frac{v_t^2}{(r^+)^2} + \frac{I^2}{4\pi^2 \sigma k (r^+)^2} + \\ \frac{N_{Pr}}{c_{p1}} \left(\frac{dv_t}{dr^+} - \frac{v_t}{r^+} \right)^2 = 0 \quad (10)$$

Equation (10) is also expressed in reduced coordinates

Electromagnetic Relationships and Power Loss

The relationship of current density, electric field, and magnetic field are found from Ohm's equation. The electrical power needed to maintain gas rotation can then be derived.

Gordeev and Gubanov have shown that, for the condition in which the ionic velocities relative to the neutral gas are much smaller than the velocity of the neutral gas, the radial components of Ohm's equation can be written as

$$j = \sigma(E + v_i B_0) \quad (11)$$

Substituting for j and v_i and integrating over r , the voltage drop across the homopole becomes, for $N_R > 0$,

$$U = \frac{I}{2\pi\sigma} \ln \frac{r_o}{r_i} + \frac{B_0^2 I r_i^2}{4\pi\mu N_R} \left\{ \frac{K_1}{N_R + 2} \left[1 - \left(\frac{r_o}{r_i} \right)^{N_R + 2} \right] - \frac{[1 - (r_o/r_i)^2]}{2} - K_2 \left(\frac{r_o}{r_i} \right)^2 \ln \frac{r}{r_i} \right\} \quad (12)$$

The corresponding expression when $N_{Re} = 0$ has been derived by Gordeev and Gubanov. Equation (12) consists of two terms: the first, involving electrical conductivity, is identified as a resistive voltage loss; the second is the additional drop, dependent on the magnetic field, necessary to maintain gas rotation. The power loss per unit of chamber length can be written immediately by multiplying both sides of Eq. (12) by I . The expression obtained is

$$P = \frac{I^2}{2\pi\sigma} \ln \frac{r_o}{r_i} + \frac{B_0^2 I^2 r_i^2}{4\pi\mu N_{Re}} \left\{ \frac{K_1}{N_{Re} + 2} \left[1 - \left(\frac{r_o}{r_i} \right)^{N_{Re} + 2} \right] - \frac{[1 - (r_o/r_i)^2]}{2} - K_2 \left(\frac{r_o}{r_i} \right)^2 \ln \frac{r}{r_i} \right\} \quad (13)$$

Total Fuel Mass

The mass of fuel inside the chamber can be obtained directly by integrating over the total volume. This is given by the expression

$$m_T = \int_0^{r_o} \int_0^L 2\pi r n_{p2} m_2 dr dz \quad (14)$$

For the case of axial concentration uniformity, Eq. (14) becomes

$$m_T = 2\pi r^2 L \int_0^1 \rho_1 \rho^{+r} dr^+ \quad (15)$$

At critical conditions, this should correspond closely to the critical mass

Method of Solution

A complete study of the system under consideration necessitates the simultaneous solution of Eqs. (2, 7, and 10) together with the velocity equation (5) and other accessory relationships. The system of equations is coupled and requires solution of three nonlinear differential equations. Such a solution is being attempted by numerical digital computer techniques. Solutions for the case not involving nuclear heating are much simpler and have been obtained for certain cases.^{8,9}

For the present paper, a simplified procedure was employed. Arbitrary temperature distributions were assumed and used to obtain solutions of the diffusion equation. Although this is not a rigorous procedure, it yields results useful for engineering approximations and at the same time greatly simplifies the treatment. The use of several temperature distributions gives some indication of their effect on rocket performance.

The three temperature distributions used are shown in Fig. 3. The distributions were chosen to give three widely varied cases. These are 1) a constant temperature, 5000°K; 2) a temperature given by the equation $T = 2000^\circ + 4000^\circ K [1 -$

$(r^+)^2]$; and 3) an arbitrary temperature with a peak of 10,000°K at $r^+ = 0.2$. The second and third cases yield wall temperatures of 2000°K.

The diffusion equation was solved as an initial boundary problem by digital computer techniques using a modified Runge-Kutta method. Integration began at the inner electrode radius i^+ and proceeded to larger radii at specified parameter values. The procedure was then repeated for other parametric values. A series of distribution curves for density ratio, velocity, propellant density, and pressure were thus obtained. A value of density ratio $\rho^+ = \rho_i^+ = 10^{-4}$ was used as the initial boundary condition on ρ^+ . This limited the solution to cases corresponding to a loss of 1 lb of fissionable fuel for every 10,000 lb of propellant. An initial value of pressure was assumed to be 1000 psi. The following other constants and parameters were used with the equations to obtain numerical answers: $m_2/m_1 = 117.5$; $I = 1000$ amp/m; $N_{Sc} = 1$; $r/r_i = 10$; and $\sigma = 1000$ mho/m.

The values of transport properties were computed at the average temperature. A value (r/r_i) of 10 corresponds to a system having an outer electrode radius ten times the inner electrode. Outer radii (r) of 2 m for the large chamber and 0.05 and 0.025 m for a system of multiple small tubes were used for comparison.

The fissionable fuel mass inside the chamber was computed from Eq. (15). This was compared with the value from nucleonics data, thus giving the critical mass as a function of parametric constants. In computing critical masses, a reactor length of 2 m was assumed. Electrical requirements were computed on the basis of the power necessary to contain a critical mass inside the chamber with negligible fuel loss. For a given critical mass, the value of $B_0 I$ determines the electrical power requirements from Eq. (13). Electrical equipment weights were estimated on the basis of 10 lb/kwe. Although this specified power is optimistic, it may well be representative of conversion equipment in the near future.

Results and Discussion

Vortex Characteristics

Figures 4-9 show typical results obtainable for a large chamber ($r_o = 2$ m). Data for small chambers followed the same trends. The density ratio distributions exhibit a simple maximum over the parametric ranges of interest to propulsion applications. Other behavior of the solutions is also possible.² For example, the case of no radial flow yields a rapidly increasing exponential distribution. For given parametric values, density ratio distributions are similar in shape, although of entirely different magnitude, for the three temperature distributions studied. In general, gas separation be-

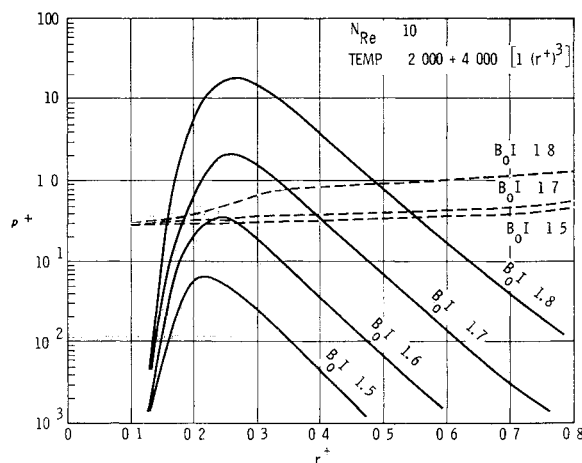


Fig. 4 Density ratio distributions in MHD vortex

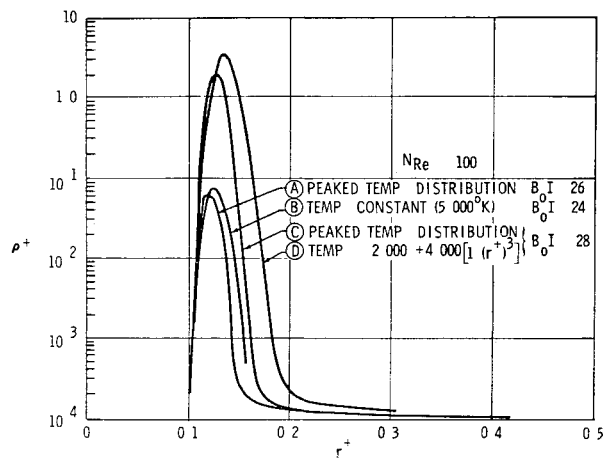


Fig 5 Effects of temperature distributions on density ratio distributions

comes more difficult as the temperature distribution becomes more complex

Increases in B_0I product increase the density ratio and shift the maximum slightly toward the outer wall. This is to be expected since increases in B_0I increase the tangential velocity, and this manifests itself as an increase in the centrifugal force, which tends to force the particles outward. On the other hand, increases in the Reynolds number shift the distribution inward toward the center electrode, narrowing it to a sharp spike (see Fig 5). This of course results from the increased drag experienced by the particles as the flow rate is increased. Since the fissionable fuel mass depends on the area under the curve, it is more difficult to obtain critical masses as Reynolds number is increased. Critical masses generally occur for ρ_m^+ values in the range of 10 to 20.

Propellant densities plotted in Fig 4 are also affected by drag and centrifugal forces, and they show an increase with increasing B_0I product. The increase is more pronounced at low values of radius ratio and tends to level off at higher values. The fissionable fuel density is readily calculable from these curves. Since the value of propellant density is approximately 1, and maximum ρ^+ is about 10, the maximum fuel density is approximately 10.

Tangential velocity distributions are shown in Fig 6 for two values of Reynolds number and several values of B_0I product. Very high tangential velocities are possible by increasing the B_0I product. The position of the maximum velocity depends on the Reynolds number. Except for very low Reynolds numbers, maximum velocity occurs very near the inner electrode. This is very significant for the separation, since a particle moving radially from outside to inside will experience the greatest centrifugal force near the inner electrode. Mach numbers for velocities of interest to economical retention depend on the Reynolds number and are in the supersonic range in the region of maximum velocity.

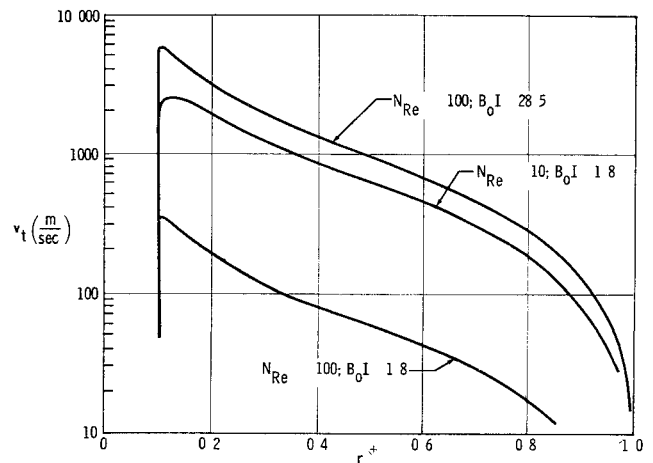


Fig 6 Tangential velocity distributions in MHD vortex

Typical pressure ratio distributions are given in Fig 7. The pressure variation was more pronounced for small r^+ because of the dependence of pressure on ρ^+ and v_t , both of which vary strongly at small values of r^+ .

Pressure ratios, periphery to core, are shown in Fig 8 as functions of B_0I product for the three temperature distributions studied. Pressure ratios increase rapidly with B_0I product, and pressure distributions vary with the choice of temperature distribution which suggests that pressure is very sensitive to variation in temperature.

Power requirements in the vortex for various Reynolds numbers are shown in Fig 10 as a function of B_0I product. These plot linearly because power is expended mainly in maintaining gas rotation [second term of Eq (13)].

Figure 10 shows typical fuel mass contained inside the chamber for a given radial Reynolds number and various temperature and design conditions. These were obtained by integrating Eq (15). The amount contained is sensitive to the B_0I value and can be increased greatly with minor changes in electrical power requirements. For the low flow rates ($N_R = -10$), the electrical requirements are not severe, but as the flow rate is increased, these increase sharply.

Engine Performance

Table 1 summarizes results of the various parametric analyses of critical reactors employing the two design concepts considered. These reactors heat a hydrogen propellant to 5000°–6000°K and thus yield specific impulses in the range of 1500–1800 sec.

The magnetic flux densities required range from a few gauss to about 1600 gauss for the plasma current density used. It is also possible to trade field strength for current density. The power required to produce these fields is negligible compared with other electrical requirements. The fields calculated here

Table 1 MHD-driven vortex nuclear reactors

r_o , m	N_{Re}	Temp, Fig 2	B_0 , webers/m ²	w , lb/m sec	Max Mach no	P , Mw/m	Elect wt, lb/m	p_0/p_1	Engine thrust/wt
2	-10	1	1.62×10^{-3}	9.8×10^{-3}	1.40	0.0023	23	1.8	2.9×10^{-4}
	-10	2	1.77×10^{-3}	9.8×10^{-3}	1.51	0.0026	26	2.0	3.4×10^{-4}
	-10	3	2.02×10^{-3}	9.8×10^{-3}	1.46	0.0034	34	2.7	2.9×10^{-4}
	-100	1	2.62×10^{-2}	9.8×10^{-2}	3.21	0.055	550	~25	2.9×10^{-3}
	-100	2	2.87×10^{-2}	9.8×10^{-2}	3.21	0.066	660	~30	3.4×10^{-3}
	-100	3	2.92×10^{-2}	9.8×10^{-2}	3.56	0.067	670	~60	2.9×10^{-3}
	-1000		0.68–0.72	9.8×10^{-1}	8.74	3.9–4.2	34,000–42,000	large	(1.6×10^{-2})
0.05 (1000 tubes)	-10	2	7.2×10^{-2}	9.8	1.44	2.8	28,000	2.5	0.22
	-10	3	8.2×10^{-2}	9.8	1.49	3.5	35,000	3.0	0.17
0.025 (3000 tubes)	-10	3	0.166	29.4	1.49	10.9	109,000	3.3	0.28

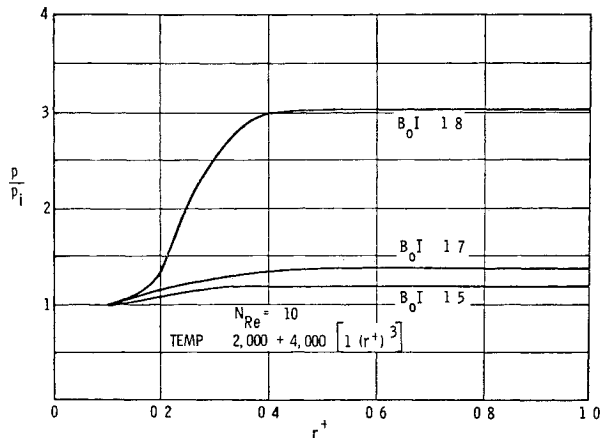


Fig 7 Pressure distributions in MHD vortex

are low when compared with fields required in the scheme of Ref 4. It should be noted, however, that in the scheme proposed here, the field is used only to drive the vortex, and gas separation results from the resulting centrifugal field. In Ref 4, a magnetic pinch is used for retainment, and the rotation is used to supplement the pinch (i.e., to drive the fuel away from the escape cone of the magnetic bottle). The use of the pinch necessitates much larger fields.

The different temperature distributions used do not significantly affect the power requirement, engine thrust-to-weight ratio, or pressure gradient (low flow rates). A constant temperature distribution yielded a good estimate of the performance. Verification of the generality of this conclusion must await solution of the coupled equations.

The results for a large chamber ($r_0 = 2$ m) show that this design is limited both by electrical power requirements and pressure gradients. Power requirements increase rapidly with flow rate. The associated electrical equipment weights, although negligible for low flow rates, become comparable to the reactor dead weight as the flow rate increases above $N_{Re} = -1000$.

The pressure penalty ratio p_0/p_i imposes a serious limitation on flow rate. These ratios increase sharply as the radial Reynolds number increases, and they rapidly get out of hand, thus limiting practical designs to low radial flow rates. This restriction cannot be alleviated by lowering the core pressure because a high core pressure is necessary to obtain criticality. The over-all net result is that thrust-to-weight ratios for practical single chambers are limited to about 10^{-4} .

Multiple-vortex reactors have several advantages over single-vortex designs. First, they improve flow rate at manageable pressure levels by increasing the effective over-all vortex length. Thus, considerable improvement in engine

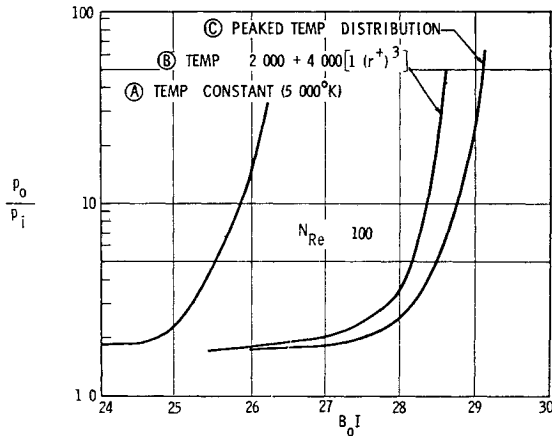


Fig 8 Effects of temperature distributions on pressure ratio

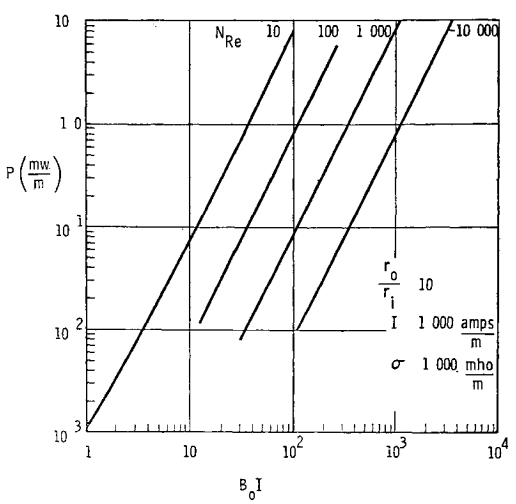


Fig 9 Electrical power requirements

thrust-to-weight ratio can be realized. Table 1 shows that thrust-to-weight ratios are in the range of tenths. Secondly, the flow conditions become less severe as the vortex radius is decreased. Whereas the maximum Reynolds number was on the order of 10^6 for the single chamber, it is on the order of 10^5 for the 0.05-m-radius vortex, and 10^4 for the 0.025-m-radius vortex.

On the other hand, multiple vortex reactors possess many disadvantages. The electrical power requirements are more severe than for a single chamber. Despite the improvement in engine thrust-to-weight ratio, this tends to nullify any advantage that these reactors might have over the purely hydrodynamic type. Also, the complexity of the electrical system for a reactor with many vortices tends to favor the hydrodynamic type. Another disadvantage, although not restricted strictly to the MHD vortex, is the more severe heat-transfer problem. The wall surface to be cooled is much larger, and fission fragment deposition at the walls can be serious, especially for tubes with diameters smaller than 2.5 cm.¹⁶

No attempt was made to maximize reactor performance by trading off nucleonic weights (dead weight) for electrical weights. However, it can be shown easily that there is little likelihood of large performance improvements. The following are two possible avenues by which performance improvements might be realized.

1) Decreasing chamber radius for constant reflector thickness: If cavity radius is decreased for a constant reflector thickness of 0.55 m, for example, it is possible to reach a minimum critical mass at a radius of about 0.5 m. Calcula-

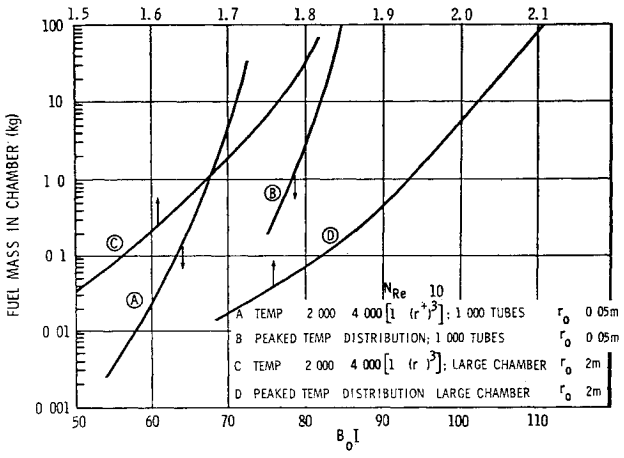


Fig 10 Fissionable fuel mass contained in MHD vortex

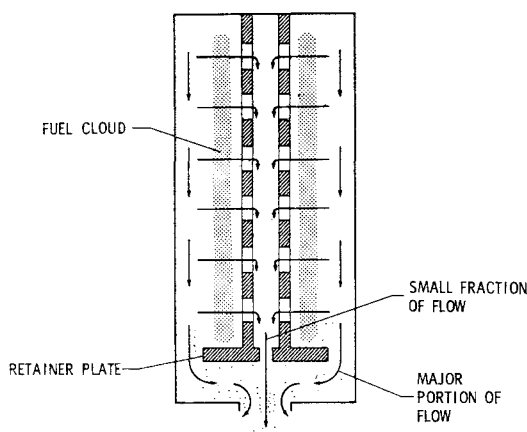


Fig. 11 Bypass flow MHD vortex concept

tions show that the single-chamber reactor thrust-to-weight ratio possibly could be increased by an order of magnitude. This improvement, however, is insufficient to put the reactor in advantageous competition with other concepts. In the case of the multiple vortex system, it is not possible to decrease the chamber radius to any large extent for the tube sizes and number assumed previously. This number of tubes already represents approximately the maximum that can be packed (with some spacing between tubes for electrical insulation) into a 2-m-radius chamber. Also it is not possible to decrease the radius of each individual tube to any large extent in order to pack more inside the chamber. As was noted before, this procedure will impose severe thermal loads at the tube walls because of fission fragment heating.

2) Decreasing reflector thickness for constant chamber radius: In this case, reactor nucleonics are worsened (because of larger critical masses), and more power will be necessary for containment. However, this is not necessarily objectionable since the fuel mass contained inside the chamber is highly sensitive to the B_0I product, and it is possible to increase the amount contained with only minor expenditure of electrical power. It is thus hoped to trade a large amount of reflector weight for a small amount of electrical weight. If the reflector thickness is decreased from 0.55 m to 0.30 m for a 2-m cavity, for example, the critical mass is increased to 70 kg. The electrical requirements to contain this larger critical mass are small, and it is possible to increase the thrust-to-weight ratio by a factor of 2 or 3. This process cannot be continued indefinitely, however. Attempts to further improve performance meet with severe pressure gradients because the pressure gradient is also highly sensitive to B_0I product.

An important consideration is the local field within the plasma under operating conditions (validity of assumption 2 in the section on Mathematical Formulation), because the fuel contained is sensitive to the local magnetic field. It is known that electromagnetic interactions induce electric currents that set up in the plasma a magnetic field opposing the applied field; it is necessary to show that the field within the plasma is constant. A useful criterion, often used to show that the induced magnetic field is negligible, is the magnetic Reynolds number. Iwellsen⁹ has shown that, to a good approximation, the axial field is given by the equation $B = B_0(1 + Nm)$. If the magnetic Reynolds number Nm is much less than 1, the internal field is nearly equal to the applied field. For the conditions presented here, Nm is on the order of 10^{-5} to 10^{-6} , so that the internal field is indeed very nearly equal to the applied field.

Two major assumptions made in this study, two-dimensionality and laminar flow, require much more study. Both of these can have serious consequences on the performance of gaseous reactors, and further consideration of this scheme must include these problems as prime study areas. As in the

case of the hydrodynamic vortex, a rigorous treatment of MHD vortex flow should be considered as a three-dimensional problem. Although it might be possible to control the type of flow somewhat by manipulating electromagnetic forces, complete two-dimensionality might be impossible. The second major assumption was that of laminar flow. The maximum Reynolds number, defined as $\rho v r_m / \mu$, is in the turbulent range for all systems studied, and the flow is supersonic. Although there are indications that the magnetic field and other forces^{2,8} tend to stabilize turbulence, there is no data to support this for the MHD vortex. Turbulence has been shown to undo the separation and thereby to hamper reactor performance. Other things being equal, however, the laminar results yield optimistic performance figures, useful at least for preliminary design and feasibility considerations. Turbulent systems are expected to worsen performance by one or two orders of magnitude.

Advanced Bypass Flow Concept

Diffusion systems restrict rocket performance primarily because of flow rate limitations. One scheme for improving engine performance employs a bypass flow concept to increase the exit flow as depicted in Fig. 11. This concept takes advantage of the possibility of concentrating the fuel in a narrow core near the central electrode (Fig. 6). In operation, a small fraction of the fuel diffuses through the fuel cloud, helping to maintain its integrity, while a major portion of the fuel bypasses around the outside and is heated by radiation. For example, if the bypassed flow is one thousand times the diffusing flow, assuming comparable reactor weights, engine thrust-to-weight ratios much greater than one are possible.

No quantitative analysis of this concept has been made at this stage. The large axial flows will introduce strong three-dimensionality into the system, and the dynamics must be considered as a three-dimensional problem. The possibility of improving the engine performance, however, merits further consideration. It might be of interest to note that bypass flow systems are also being considered for improving the performance of hydrodynamic containment schemes.

Conclusions

Analysis of the two-dimensional MHD vortex has shown it to be capable of high tangential velocities. Two gases of greatly varying mass can be separated in a radially diffusing system so that the heavy gas is strongly concentrated near the central electrode.

Practical application of this type of vortex to fuel containment in gaseous core nuclear engine designs indicates that the concept is limited to low flow rates by high electrical requirements and severe pressure penalties. The engine thrust-to-weight ratio is about 10^{-4} for a single chamber design. The multiple vortex design is also limited by large electrical requirements and more complex design problems. Engine thrust-to-weight ratios are on the order of tenths. Large improvements in performance seem unlikely with the diffusion-type systems considered, and if turbulence is shown to be present, even poorer performance can be expected.

The bypass flow concept is suggested as a means of alleviating the main restriction imposed on diffusing systems, i.e., flow rate. Improvement in engine performance is possible in principle with this scheme, and the system merits further study.

References

- 1 Grey, J., "A gaseous core nuclear rocket utilizing hydrodynamic containment of fissionable material," ARS Preprint 848 59 (June 1959).
- 2 Kerrebrock, J. L. and Meghrebian, R. V., "An analysis of vortex tubes for combined gas phase fission heating and separa-

tion of the fissionable material," Oak Ridge National Lab CF-57-11 3, Revision 1, Oak Ridge, Tenn (April 11, 1958)

³ McKee, J W , "The glow-plug gas-core reactor " Gaseous Fission Reactors Symposium, Pasadena, Calif (April 26-27, 1962)

⁴ Nelson, S T , "The plasma core reactor," ARS Preprint 1734 61 (May 1961)

⁵ Rosa, R J , "A propulsion system using a cavity reactor and magnetohydrodynamic generator," ARS Preprint 1519 60 (December 1960)

⁶ Weinstein, H and Ragsdale, R G , "A coaxial flow reactor—A gaseous nuclear rocket concept," ARS Preprint 1518-60 (December 1960)

⁷ Romero, J B , "Fuel containment in the gaseous-core nuclear rocket by MHD driven vortices," Boeing Co Doc D2-22408 (March 4, 1963); also presented at the Fiftieth National Meeting of the American Institute of Chemical Engineers, Buffalo, N Y (May 5-8, 1963)

⁸ Gordeev, G V and Gubanov, A I , "Acceleration of a plasma in a magnetic field," Soviet Phys **3**, 1880-1887 (1958)

⁹ Lewellen, W S , "Magnetohydrodynamically driven vortices," *Proceedings of the 1960 Heat Transfer and Fluid Mechanics Institute* (Stanford University Press, Stanford, Calif, 1960), pp 1-15

¹⁰ Anderson, O , Baker, W R ,¹Bratenahl, A , Furth, H P , and Kunkel, W B , "A hydromagnetic capacitor," J Appl Phys **30**, 188-196 (1959)

¹¹ Early, H C and Dow, W G , "A cross field ionic wind motor," *Conference on Extremely High Temperature* (John Wiley and Sons, Inc , New York, 1958), pp 187-193

¹² Bishop, A S , *Project Sherwood—The U S Program in Controlled Fusion* (Addison-Wesley Publishing Co , Inc , Reading, Mass , 1958), pp 128-131

¹³ Safonov, G , "Externally moderated reactors," *Proceedings of the Second United Nations International Conference on Peaceful Uses of Atomic Energy* (United Nations, Geneva, 1958), Vol 12, pp 705-718

¹⁴ Chapman, S and Cowling, T G , *The Mathematical Theory of Non-Uniform Gases* (Cambridge University Press, Cambridge, England, 1960), Chap 14

¹⁵ Rosenweig, M L , Lewellen, W S , and Kerrebrock, J L , "The feasibility of turbulent vortex containment in the gaseous fission rocket," ARS Preprint 1516A-60 (December 1960)

¹⁶ Stumpf, H J , "Fission fragment energy loss from vortex tubes," Jet Propulsion Lab Tech Rept 32-188 (March 12, 1962)